GEOLOGY | THE GEOLOGICAL SOCIETY OF AMERICA®

https://doi.org/10.1130/G46275.1

Manuscript received 19 December 2018
Revised manuscript received 29 April 2019
Manuscript accepted 29 April 2019

Supereruption quartz crystals and the hollow reentrants

Kenneth S. Befus[1] and Michael Manga[2]
[1]Department of Geosciences, Baylor University, Waco, Texas 76798, USA
[2]Department of Earth and Planetary Science, University of California, Berkeley, California 94720, USA

ABSTRACT

Hollow reentrants in quartz phenocrysts from Yellowstone (western United States) caldera's Lava Creek Tuff are preserved vestiges of bubbles in the supereruption's pre-eruptive magma reservoir. We characterized the reentrants using a combination of petrographic techniques, synchrotron X-ray microtomography, and cathodoluminescence imagery. One or more reentrants occur in ~20% of quartz, and up to ~90% of those reentrants are hollow. The earliest-erupted parts of the Lava Creek Tuff have the most empty reentrants. The hollow reentrants provide direct, physical evidence for volatile saturation, exsolution, and retention in a magma reservoir. Quartz-melt surface tension permits bubbles to attach to quartz only when bubbles have been able to nucleate and grow in the melt. Prior to eruption, the Lava Creek Tuff existed as a bubbly, volatile-saturated magma reservoir. The exsolved volatiles increased magma compressibility, helping to prevent the ever-accumulating magma from reaching a critical, eruptive overpressure until it reached a tremendous volume.

INTRODUCTION

Volcanic gases provide the driving force for explosive volcanism (Cassidy et al., 2018). These gases exsolve from the melt when it becomes saturated, most commonly in response to decompression during eruptive ascent (Edmonds, 2008). The timing and nature of volatile exsolution during an eruption control many variables, including style, explosivity, and ascent rate. Remotely sensed measurements of such atmospheric release identified "excess sulfur" in the 1991 Pinatubo eruption plume, revealing that magmas may be saturated prior to eruption and may contain an exsolved fluid as bubbles (Gerlach et al., 1996). The eruption of Pinatubo confirmed previous research that reasoned that bubbles may indeed exist in the magma reservoir, sometimes in significant volume (e.g., Roedder, 1965; Anderson, 1991; Tait, 1992; Lowenstern, 1995; Wallace et al., 1995).

Many observations now exist to geochemically establish pre-eruptive volatile saturation, or lack thereof (Edmonds and Woods, 2018). Excess sulfur has been documented via remote sensing at other volcanoes, including El Chichón (Mexico), Mount St. Helens (Washington State, USA), and Mount Redoubt (Alaska, USA) (Gerlach and McGee, 1994; Gerlach et al., 1994, 1996). The volatile and trace element concentrations of melt inclusions present compositional trends that suggest saturation (Luhr, 1990; Wallace et al., 1995). Metal scavenging by convecting, pre-eruptive bubbles is a mechanism for generation of economically valuable magmatic porphyry ore deposits (Waite et al., 1997; Cloos, 2001; Vigneresse et al., 2019). Exsolved fluids from depth may also flux through shallow portions of an interconnected magmatic plumbing system (Rust et al., 2004; Lowenstern and Hurwitz, 2008; Caricchi et al., 2018). These geochemical lines of evidence each provide a strong case for pre-eruptive saturation.

Exsolved fluid has meaningful consequences for diverse magmatic and eruption processes. Chief among them is the triggering of eruptions, because the exsolved fluid contributes to melt buoyancy and reservoir overpressure (Caricchi et al., 2014; Degruyter and Huber, 2014; Malfait et al., 2014). After an eruption initiates, pre-eruptive bubbles modify degassing behavior in the conduit and thus influence melt viscosity, ascent rates, and fragmentation (Gonnermann and Manga, 2007; Giordano et al., 2008; Gardner, 2009). Assumptions regarding volatile saturation also have important petrologic consequences in the pre-eruptive reservoir. The existence of exsolved gas in a melt would alter the volume change of phase equilibrium reactions, thereby shifting the thermodynamic stability fields of mineral phases, and influence our ability to use thermobarometers to understand magma storage conditions (e.g., Ghiorso and Evans, 2008; Putirka, 2008; Gualda et al., 2012).

Here, we report a direct, physical record of pre-eruptive saturation and fluid exsolution for the magma of the Lava Creek Tuff, emplaced during the most recent supereruption from Yellowstone caldera, western United States (Christiansen, 2001; Shamloo and Till, 2019). Lava Creek Tuff is one of the few eruptions from Yellowstone caldera that contains hydrous mineral phases (Christiansen, 2001). But the record of volatile saturation is preserved in quartz, one of its anhydrous phases. Quartz crystals from the Lava Creek Tuff are pervasively riddled with tortuous to simple-shaped reentrants. Many of those quartz-hosted reentrants are hollow.

The absence of glass in the Lava Creek Tuff reentrants was an unforeseen discovery. Glass-filled reentrants, sometimes called embayments, are features that have been used to understand magmatism at Yellowstone and elsewhere (e.g., Anderson, 1991; Liu et al., 2006; Loewen and Bindeman, 2015; Myers et al., 2016, 2018). They provide a useful geospeedometer because the glass preserves a record of the diffusion-limited re-equilibration of volatiles during magmatic ascent (e.g., Liu et al., 2007; Humphreys et al., 2008; Lloyd et al., 2014; Ferguson et al., 2016; Myers et al., 2016, 2018). The empty reentrants in the Lava Creek Tuff instead provide insight into magma reservoir processes when quartz crystals were growing.

The quartz-hosted empty reentrants in the Lava Creek Tuff preserve the vestiges of pre-eruptive bubbles once filled with exsolved fluids. The dimensions and numbers of the empty reentrants provide the first estimate (a minimum) for the amount of bubbles in the reservoir prior to eruption. Increased magma compressibility is one critical implication of the exsolved fluids within the magma. We propose that compressibility likely allowed the Lava Creek Tuff magma to more readily accommodate recharge events, which allowed the chamber to grow to a large volume before eruption (Degruyter and Huber, 2014).

METHODS AND RESULTS

Pumice clasts were collected from outcrops of the poorly welded base and welded interior of the Lava Creek Tuff A ignimbrite, as well

CITATION: Befus, K.S., and Manga, M., 2019, Supereruption quartz crystals and the hollow reentrants: Geology, https://doi.org/10.1130/G46275.1

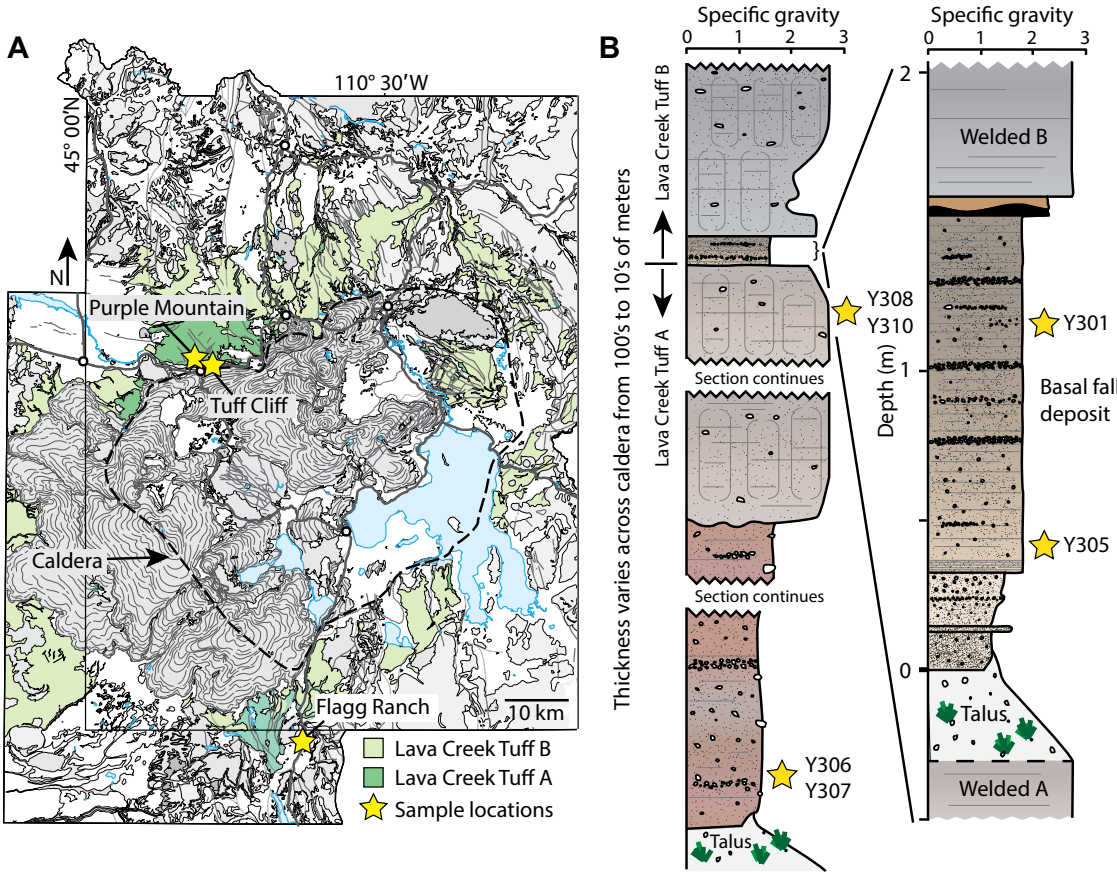

Figure 1. A: Geologic map of sample locations in Yellowstone National Park, western United States, and surrounding region; modified from Christiansen (2001). The extent of Lava Creek Tuff deposits are highlighted in green. Gray domains with curved lines are post-caldera rhyolites with pressure ridges shown schematically (Christiansen 2000). Blue domains are lakes and rivers. The remaining white areas are undifferentiated recent alluvial sediments or pre-Lava Creek Tuff deposits. B: Schematic measured section shows relative stratigraphic position of pumice samples. Pumice, lapilli, and gray bedding planes are illustrated schematically. Colors were chosen to best represent the color of observed outcrop variations, but should also be considered schematic.

as from the unwelded basal fall layer of Lava Creek Tuff B (Fig. 1). Basal falls would have been the preferred material to collect for Lava Creek Tuff A, but outcrops remain unknown. The pumices were crushed, sieved, and hand-picked to make quartz mineral separates. Quartz occur as euhedral bipyramids, or partial crystals with some faceted faces. Almost every crystal contains glass-filled, enclosed melt inclusions. The crystals are also embayed with one or more reentrants. Many of these reentrants are empty void space, not filled with glass.

To establish the statistical significance of the empty reentrants across the Lava Creek Tuff, we surveyed a few thousand quartz crystals and their reentrants from pumice samples (Table 1). We selected characteristic reentrant-bearing quartz crystals for synchrotron X-ray microtomography (μXRT) and cathodoluminescence (CL) analyses to establish the relationship between the reentrants and crystallization processes (see the GSA Data Repository[1]). Reentrants are most common in the earliest-erupted Lava Creek Tuff A (Table 1). They occur in one-quarter of the quartz crystals, and >80% of those are hollow. Reentrants become slightly less common upsection, appearing in ~20% of quartz crystals from pumices in the middle and upper portions of the ignimbrite. Reentrant filling is variable in those samples, with some primarily filled with glass whereas they are almost all empty in other samples. Quartz from the basal fall of Lava Creek Tuff B contains reentrants in ~18% of the crystals.

Empty reentrants account for 0.02–1.5 vol% of their host quartz crystals. They appear as embayments or tubes ranging from a few microns to 400 μm wide that extend into the center of the crystals (Fig. DR1 in the Data Repository). They are locally bulbous with bulging interiors that narrow to necks at the crystal surface. "Penetration" depth is highly variable, extending as far as 1600 μm, although most range from 50 to 500 μm. Rare embayments tunnel through entire crystals, creating hollow pathways that connect opposite faces (Fig. 2; Videos DR4–DR8). Many reentrants discordantly cut across primary growth bands in quartz, which appear as alternating light and dark bands in CL (Fig. 2). CL images constrain the relative timing of quartz growth and the reentrants.

Empty reentrants sometimes contain magnetite crystals up to 50 μm in diameter, as well as small pockets of glass adhered to reentrant walls (Fig. 2). Reentrant shape does not correlate with its emptiness. In a given sample, both tortuous and simple-shaped reentrants may be hollow or filled with glass.

DISCUSSION

To infer the significance of the empty reentrants, we must consider how they came to be. Previous work regarding reentrants describes

TABLE 1. REENTRANT AND INCLUSION ABUNDANCES FOR LAVA CREEK TUFF A AND B, YELLOWSTONE, WESTERN USA

Eruption	Sample	Percent with melt inclusions (%)	Percent reentrants (%)	Percent empty reentrants (%)	*n*
Lava Creek Tuff A	Y306	95	26	87	728
	Y307	93	23	84	1405
	Y308	97	21	11	831
	Y310	96	20	94	498
Lava Creek Tuff B	Y301	93	18	62	608
	Y305	92	18	16	630

Note: n is the total number of counted quartz crystals in each sample, with ~4700 crystals examined across all samples. Repeated counts on the same population produced counting errors of <1%.

[1]GSA Data Repository item 2019256, Figures DR1 and DR2 (additional quartz surface and reentrant textures), Figure DR3 (describing the effect of gas on magma compressibility), and Videos DR4–DR8 (3-D X-ray scans of the quartz and reentrants), is available online at http://www.geosociety.org/datarepository/2019/, or on request from editing@geosociety.org.

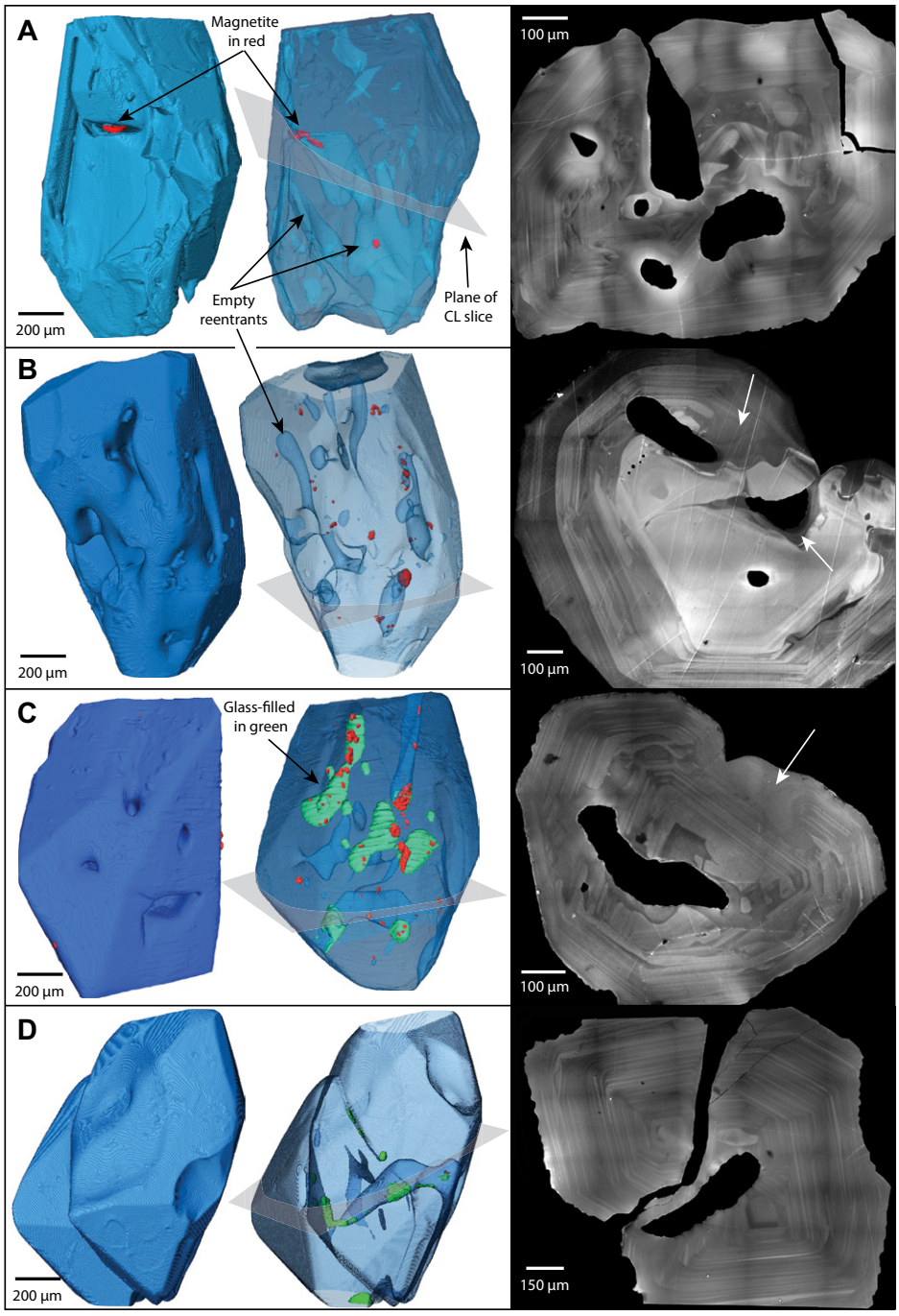

Figure 2. Synchrotron X-ray microtomography (µXRT) and cathodoluminescence (CL) images of quartz from Lava Creek Tuff, Yellowstone, western United States. µXRT images (left) are shown both with opaque and transparent surfaces to show surface morphology and interior distribution of reentrants (blue pathways). Magnetite and glass are shown in red and green, respectively. CL images (right) display crystal interior along slice plane shown in gray on transparent surface in µXRT images. Growth bands display prominent grayscale differences. White arrows highlight quartz partially to completely filling earlier reentrants.

them being filled with dense glass that preserves volatile diffusion profiles that are enriched in the interior and decrease systematically toward the outlet (e.g., Liu et al., 2007; Humphreys et al., 2008; Lloyd et al., 2014). Commonly, a single, outsized bubble occurs at the crystal-melt interface, which acts as the sink for the degassing volatiles.

Empty reentrants require a different mechanism of formation. They were either initially filled with melt that was subsequently expelled by vesiculation, or primarily filled with exsolved fluid. During decompression, the expanding fluid would force out melt, but that mechanism is not preferred because when glass is preserved, it is not highly vesiculated. Further, it is unlikely that pumiceous, inflating melt responding to decompression would expand efficiently through tortuous and irregular pathways to produce evacuated, clean reentrants. Instead, formation could occur via dissolution or by synchronous growth, if the fluid exsolved at a similar rate to quartz growth (Gutmann, 1974).

The dissolution model is supported by textures preserved within the crystals. Many reentrants crosscut CL bands (Fig. 2). Most of the reentrants are interpreted to have formed by local, accelerated dissolution of quartz by pre-eruptive bubbles (Busby and Barker, 1966; Gutmann, 1974; Donaldson and Henderson, 1988). Accelerated dissolution has been documented experimentally and is inferred to be driven by local thermodynamic disequilibrium and enhanced molecular transport along the fluid-melt interface (Busby and Barker, 1966) (Fig. DR2). This process of dissolution in the presence of bubbles of exsolved fluid was ongoing during the crystallization of quartz. We see evidence for bubble departure, as some crystals contain early-generation reentrants in their interiors that crosscut CL bands from earlier growth, but were later filled with quartz (Fig. 2).

Quartz-hosted, glass-filled reentrants cut across CL bands in eruptions from other calderas, including the Toba Tuff (Indonesia), the Oruanui Tuff (New Zealand), and the Central Plateau Member rhyolite lavas (Yellowstone caldera) (Liu et al., 2006; Vazquez et al., 2009; Girard and Stix, 2010; Matthews et al., 2012; Loewen and Bindeman, 2015). In these examples, melt filled the reentrants. The dissolution to produce those reentrants may provide evidence that those magmas contained exsolved fluid bubbles at one time. Indeed, volatile saturation is proposed for those and many other large silicic eruptions. For example, the Bishop Tuff (California) is estimated to have been volatile-stratified, with its upper portions containing at least 3 wt% exsolved gas, equivalent to 5–20 vol% exsolved fluid (Wallace et al., 1995). Primary bubbles in reentrants from the Bishop Tuff provide additional physical evidence that the magma contained an exsolved fluid (Anderson, 1991).

Primary, magmatic fluid inclusions composed of H_2O-CO_2 mixtures are sometimes preserved in phenocrysts from volcanic eruptions (e.g., Lowenstern, 2003; Kamenetsky and Kamenetsky, 2010; Audétat and Lowenstern, 2014). These "voids" within crystals preserve a record of pre-eruptive exsolved volatiles. Magmatic fluid inclusions are commonly used as observational data sets to understand the fluids supplied to magmatic ore deposits (e.g., Heinrich et al., 1999). They are less commonly discussed in the volcanic context, but are similar to established intrusive features such as miarolitic cavities (e.g., Kamenetsky et al. 2002). Volcanic, primary fluid inclusions have been described in

different mineral phases crystallized from a diverse array of mafic to silicic eruptions (olivine: Roedder, 1965; plagioclase: Gutmann, 1974; Naumov et al., 1996; quartz: Davidson and Kamenetsky, 2007; Pasteris et al., 1996). Indeed, Gutmann (1974) described some fluid inclusions as "tubular voids" that are open at the surface of the crystal, similar to the reentrants described here.

The empty, quartz-hosted reentrants are a new example of magmatic fluid inclusions that provides a physical record of exsolved volatiles in the Lava Creek Tuff reservoir. We theorize that the hollow reentrants were filled with exsolved volatiles in the pre-eruptive magma, and can be considered quartz-hosted "bubbles." Bubbles demonstrate that the magma was saturated prior to eruption. But how bubbly was the magma? Empty reentrants occupy 0.02–1.5 vol% of the host quartz. Reentrants from the basal ignimbrite of the earliest-erupted Lava Creek Tuff occupy the most volume, accounting for 0.4 ± 0.4 vol% of the quartz. Throughout the Lava Creek Tuff, ~15%–25% of quartz crystals contain embayments. Quartz is a common phenocryst, but accounts for only ~10 vol% of the dense rock. Reentrants thus represent a tiny percentage of magma, <0.03 vol%. But, the number and volume of quartz-hosted reentrants is a strict minimum for the pre-eruptive bubble content; the total exsolved fluid must have been much higher.

Bubbles preferentially nucleate on crystal surfaces because reduced surface tension lowers the required supersaturation (Hurwitz and Navon, 1994). Magnetite crystals significantly drop the required supersaturation, making them an excellent heterogeneous nucleation surface for bubbles (Gardner, 2007). Quartz surfaces do not strongly encourage bubble nucleation (Cluzel et al., 2008). Texturally, we know that bubbles must have attached to quartz in order to drill the reentrants via dissolution. These were large bubbles whose size likely correlates with reentrant diameter (10–400 µm wide). Smaller bubbles may have been established on oxide crystals. This creates a picture of the pre-eruptive magma: large, free-floating bubbles were distributed throughout the Lava Creek magma, some preferentially attaching to quartz and other phenocryst phases.

We cannot constrain the absolute abundance of exsolved magmatic volatiles in the Lava Creek Tuff. The reentrants demonstrate that the magma was saturated, with more exsolved fluid likely in the upper portions of the reservoir, but the empty reentrants provide only a lower bound. Nevertheless, the textures record retained exsolved volatiles in the magma, complementing both geodetic measurements that indicate that exsolved volatiles are present in magmatic reservoirs, and the geochemical evidence for volatile exsolution (Kilbride et al., 2016). Surface gas flux measurements demonstrate that the modern Yellowstone magmatic system is likely gas saturated (Lowenstern and Hurwitz, 2008). Gassy magma has different physical properties than volatile-undersaturated melt. Of particular importance is the compressibility of magma because it affects the evolution of magma pressure and the volume of magma that will erupt (Edmonds and Woods, 2018).

Our results have bearing on what may make eruptions super. There are two key questions. First, why do large volumes of magma accumulate before eruption? Second, why are the eruptions themselves so large? The presence of exsolved volatiles greatly increases magma compressibility (Fig. DR3). In turn, high compressibility buffers magma reservoirs from large changes in overpressure during recharge events (Townsend et al., 2019). High compressibility also promotes eruptions that are long lived and discharge a greater proportion of stored magma (Huppert and Woods, 2002). Our measurements directly document the existence of exsolved volatiles in the reservoirs that supplied supereruptions.

ACKNOWLEDGMENTS

We thank Rachel Bruyere for assistance in the field and sample preparation. We also thank Madison Myers, Jacob Lowenstern, and Eric Christiansen for thorough reviews. CL imagery was collected with the assistance of James Maner at University of Texas at Austin (USA). This research was supported by National Science Foundation grants EAR-1724429 to Befus and EAR-1724469 to Manga. This research used beamline 8.3.2 of the Advanced Light Source (Lawrence Berkeley National Laboratory, Berkeley, California), which is a Department of Energy Office of Science User Facility under contract DE-AC02–05CH11231. We thank Dula Parkinson for help with the µXRT imaging and analysis.

REFERENCES CITED

Anderson, A.T., Jr., 1991, Hourglass inclusions: Theory and application to the Bishop Rhyolitic Tuff: American Mineralogist, v. 76, p. 530–547.

Audétat, A., and Lowenstern, J.B., 2014, Melt inclusions, *in* Holland, H.D., and Turekian, K.K., eds., Treatise on Geochemistry (second edition): Oxford, UK, Elsevier, p. 143–173, https://doi.org/10.1016/B978-0-08-095975-7.01106-2.

Busby, T.S., and Barker, J., 1966, Simulative studies of upward drilling: Journal of the American Ceramic Society, v. 49, p. 441–446, https://doi.org/10.1111/j.1151-2916.1966.tb15413.x.

Caricchi, L., Annen, C., Blundy, J., Simpson, G., and Pinel, V., 2014, Frequency and magnitude of volcanic eruptions controlled by magma injection and buoyancy: Nature Geoscience, v. 7, p. 126–130, https://doi.org/10.1038/ngeo2041.

Caricchi, L., Sheldrake, T.E., and Blundy, J., 2018, Modulation of magmatic processes by CO_2 flushing: Earth and Planetary Science Letters, v. 491, p. 160–171, https://doi.org/10.1016/j.epsl.2018.03.042.

Cassidy, M., Manga, M., Cashman, K., and Bachmann, O., 2018, Controls on explosive-effusive volcanic eruption styles: Nature Communications, v. 9, 2839, https://doi.org/10.1038/s41467-018-05293-3.

Christiansen, R. L., 2001, The Quaternary and Pliocene Yellowstone Plateau volcanic field of Wyoming, Idaho, and Montana: U. S. Geological Survey Professional Paper 729-G, 120 p., https://pubs.usgs.gov/pp/pp729g/pp729g.pdf.

Cloos, M., 2001, Bubbling magma chambers, cupolas, and porphyry copper deposits: International Geology Review, v. 43, p. 285–311, https://doi.org/10.1080/00206810109465015.

Cluzel, N., Laporte, D., Provost, A., and Kannewischer, I., 2008, Kinetics of heterogeneous bubble nucleation in rhyolitic melts: Implications for the number density of bubbles in volcanic conduits and for pumice textures: Contributions to Mineralogy and Petrology, v. 156, p. 745–763, https://doi.org/10.1007/s00410-008-0313-1.

Davidson, P., and Kamenetsky, V.S., 2007, Primary aqueous fluids in rhyolitic magmas: Melt inclusion evidence for pre-and post-trapping exsolution: Chemical Geology, v. 237, p. 372–383, https://doi.org/10.1016/j.chemgeo.2006.07.009.

Degruyter, W., and Huber, C., 2014, A model for eruption frequency of upper crustal silicic magma chambers: Earth and Planetary Science Letters, v. 403, p. 117–130, https://doi.org/10.1016/j.epsl.2014.06.047.

Donaldson, C.H., and Henderson, C.M.B., 1988, A new interpretation of round embayments quartz crystals: Mineralogical Magazine, v. 52, p. 27–33, https://doi.org/10.1180/minmag.1988.052.364.02.

Edmonds, M., 2008, New geochemical insights into volcanic degassing: Philosophical Transactions of the Royal Society of London A: Mathematical, Physical and Engineering Sciences, v. 366, p. 4559–4579, https://doi.org/10.1098/rsta.2008.0185.

Edmonds, M., and Woods, A.W., 2018, Exsolved volatiles in magma reservoirs: Journal of Volcanology and Geothermal Research, v. 368, p. 13–30, https://doi.org/10.1016/j.jvolgeores.2018.10.018.

Ferguson, D.J., Gonnermann, H.M., Ruprecht, P., Plank, T., Hauri, E.H., Houghton, B.F., and Swanson, D.A., 2016, Magma decompression rates during explosive eruptions of Kīlauea volcano, Hawaii, recorded by melt embayments: Bulletin of Volcanology, v. 78, 71, https://doi.org/10.1007/s00445-016-1064-x.

Gardner, J.E., 2007, Heterogeneous bubble nucleation in highly viscous silicate melts during instantaneous decompression from high pressure: Chemical Geology, v. 236, p. 1–12, https://doi.org/10.1016/j.chemgeo.2006.08.006.

Gardner, J.E., 2009, The impact of pre-existing gas on the ascent of explosively erupted magma: Bulletin of Volcanology, v. 71, p. 835–844, https://doi.org/10.1007/s00445-009-0276-8.

Gerlach, T.M., and McGee, K.A., 1994, Total sulfur dioxide emissions and pre-eruption vapor-saturated magma at Mount St. Helens, 1980–88: Geophysical Research Letters, v. 21, p. 2833–2836, https://doi.org/10.1029/94GL02761.

Gerlach, T.M., Westrich, H.R., Casadevall, T.J., and Finnegan, D.L., 1994, Vapor saturation and accumulation in magmas of the 1989–1990 eruption of Redoubt Volcano, Alaska: Journal of Volcanology and Geothermal Research, v. 62, p. 317–337, https://doi.org/10.1016/0377-0273(94)90039-6.

Gerlach, T.M., Westrich, H.R., and Symonds, R.B., 1996, Preeruption vapor in magma of the climactic Mount Pinatubo eruption: Source of the giant stratospheric sulfur dioxide cloud, *in* Newhall, C.G., and Punongbayan, R.S., eds., Fire and Mud: Eruptions and Lahars of Mount Pinatubo, Philippines: Seattle, University of Washington Press, p. 415–433.

Ghiorso, M.S., and Evans, B.W., 2008, Thermodynamics of rhombohedral oxide solid solutions and a revision of the Fe-Ti two-oxide geothermometer and oxygen-barometer: American Journal of

Science, v. 308, p. 957–1039, https://doi.org/10.2475/09.2008.01.
Giordano, D., Russell, J.K., and Dingwell, D.B., 2008, Viscosity of magmatic liquids: A model: Earth and Planetary Science Letters, v. 271, p. 123–134, https://doi.org/10.1016/j.epsl.2008.03.038.
Girard, G., and Stix, J., 2010, Rapid extraction of discrete magma batches from a large differentiating magma chamber: The Central Plateau Member rhyolites, Yellowstone Caldera, Wyoming: Contributions to Mineralogy and Petrology, v. 160, p. 441–465, https://doi.org/10.1007/s00410-009-0487-1.
Gonnermann, H.M., and Manga, M., 2007, The fluid mechanics inside a volcano: Annual Review of Fluid Mechanics, v. 39, p. 321–356, https://doi.org/10.1146/annurev.fluid.39.050905.110207.
Gualda, G.A., Ghiorso, M.S., Lemons, R.V., and Carley, T.L., 2012, Rhyolite-MELTS: A modified calibration of MELTS optimized for silica-rich, fluid-bearing magmatic systems: Journal of Petrology, v. 53, p. 875–890, https://doi.org/10.1093/petrology/egr080.
Gutmann, J.T., 1974, Tubular voids within labradorite phenocrysts from Sonora, Mexico: American Mineralogist, v. 59, p. 666–672.
Heinrich, C.A., Günther, D., Audétat, A., Ulrich, T., and Frischknecht, R., 1999, Metal fractionation between magmatic brine and vapor, determined by microanalysis of fluid inclusions: Geology, v. 27, p. 755–758, https://doi.org/10.1130/0091-7613(1999)027<0755:MFBMBA>2.3.CO;2.
Humphreys, M.C.S., Menand, T., Blundy, J.D., and Klimm, K., 2008, Magma ascent rates in explosive eruptions: Constraints from H_2O diffusion in melt inclusions: Earth and Planetary Science Letters, v. 270, p. 25–40, https://doi.org/10.1016/j.epsl.2008.02.041.
Huppert, H.E., and Woods, A.W., 2002, The role of volatiles in magma chamber dynamics: Nature, v. 420, p. 493–495, https://doi.org/10.1038/nature01211.
Hurwitz, S., and Navon, O., 1994, Bubble nucleation in rhyolitic melts: Experiments at high pressure, temperature, and water content: Earth and Planetary Science Letters, v. 122, p. 267–280, https://doi.org/10.1016/0012-821X(94)90001-9.
Kamenetsky, V.S., van Achterbergh, E., Ryan, C.G., Naumov, V.B., Mernagh, T.P., and Davidson, P., 2002, Extreme chemical heterogeneity of granite-derived hydrothermal fluids: An example from inclusions in a single crystal of miarolitic quartz: Geology, v. 30, p. 459–462, https://doi.org/10.1130/0091-7613(2002)030<0459:ECHOGD>2.0.CO;2.
Kamenetsky, V.S., and Kamenetsky, M.B., 2010, Magmatic fluids immiscible with silicate melts: Examples from inclusions in phenocrysts and glasses, and implications for magma evolution and metal transport: Geofluids, v. 10, p. 293–311, https://doi.org/10.1111/j.1468-8123.2009.00272.x.
Kilbride, B.M., Edmonds, M., and Biggs, J., 2016, Observing eruptions of gas-rich compressible magmas from space: Nature Communications, v. 7, 13744, https://doi.org/10.1038/ncomms13744.
Liu, Y., Anderson, A.T., Wilson, C.J., Davis, A.M., and Steele, I.M., 2006, Mixing and differentiation in the Oruanui rhyolitic magma, Taupo, New Zealand: Evidence from volatiles and trace elements in melt inclusions: Contributions to Mineralogy and Petrology, v. 151, p. 71–87, https://doi.org/10.1007/s00410-005-0046-3.
Liu, Y., Anderson, A.T., and Wilson, C.J., 2007, Melt pockets in phenocrysts and decompression rates of silicic magmas before fragmentation: Journal of Geophysical Research, v. 112, B06204, https://doi.org/10.1029/2006JB004500.
Lloyd, A.S., Ruprecht, P., Hauri, E.H., Rose, W., Gonnermann, H.M., and Plank, T., 2014, NanoSIMS results from olivine-hosted melt embayments: Magma ascent rate during explosive basaltic eruptions: Journal of Volcanology and Geothermal Research, v. 283, p. 1–18, https://doi.org/10.1016/j.jvolgeores.2014.06.002.
Loewen, M.W., and Bindeman, I.N., 2015, Oxygen isotope and trace element evidence for three-stage petrogenesis of the youngest episode (260–79 ka) of Yellowstone rhyolitic volcanism: Contributions to Mineralogy and Petrology, v. 170, 39, https://doi.org/10.1007/s00410-015-1189-5.
Lowenstern, J.B., 1995, Applications of silicate-melt inclusions to the study of magmatic volatiles, *in* Thompson, J.F.H., ed., Magmas, Fluids, and Ore Deposits: Mineralogical Association of Canada Short Course 23, p. 71–99.
Lowenstern, J.B., 2003, Melt inclusions come of age: Volatiles, volcanoes, and Sorby's legacy, *in* De Vivo, B., and Bodnar, R.J., eds., Melt Inclusions in Volcanic Systems: Methods, Applications and Problems: Developments in Volcanology, v. 5, p. 1–21, https://doi.org/10.1016/S1871-644X(03)80021-9.
Lowenstern, J.B., and Hurwitz, S., 2008, Monitoring a supervolcano in repose: Heat and volatile flux at the Yellowstone Caldera: Elements, v. 4, p. 35–40, https://doi.org/10.2113/GSELEMENTS.4.1.35.
Luhr, J.F., 1990, Experimental phase relations of water- and sulfur-saturated arc magmas and the 1982 eruptions of El Chichón volcano: Journal of Petrology, v. 31, p. 1071–1114, https://doi.org/10.1093/petrology/31.5.1071.
Malfait, W.J., Seifert, R., Petitgirard, S., Perrillat, J.-P., Mezouar, M., Ota, T., Nakamura, E., Lerch, P., and Sanchez-Valle, C., 2014, Supervolcano eruptions driven by melt buoyancy in large silicic magma chambers: Nature Geoscience, v. 7, p. 122–125, https://doi.org/10.1038/ngeo2042.
Matthews, N.E., Smith, V.C., Costa, A., Durant, A.J., Pyle, D.M., and Pearce, N.J.G., 2012, Ultra-distal tephra deposits from super-eruptions: Examples from Toba, Indonesia and Taupo Volcanic Zone, New Zealand: Quaternary International, v. 258, p. 54–79, https://doi.org/10.1016/j.quaint.2011.07.010.
Myers, M.L., Wallace, P.J., Wilson, C.J., Morter, B.K., and Swallow, E.J., 2016, Prolonged ascent and episodic venting of discrete magma batches at the onset of the Huckleberry Ridge supereruption, Yellowstone: Earth and Planetary Science Letters, v. 451, p. 285–297, https://doi.org/10.1016/j.epsl.2016.07.023.
Myers, M.L., Wallace, P.J., and Wilson, C.J., 2018, Inferring magma ascent timescales and reconstructing conduit processes in explosive rhyolitic eruptions using diffusive losses of hydrogen from melt inclusions: Journal of Volcanology and Geothermal Research, v. 369, p. 95–112, https://doi.org/10.1016/j.jvolgeores.2018.11.009.
Naumov, V.B., Tolstykh, M.L., Kovalenker, V.A., and Kononkova, N.N., 1996, Fluid overpressure in andesite melts from central Slovakia: Evidence from inclusions in minerals: Petrology, v. 4, p. 265–276.
Pasteris, J.D., Wopenka, B., Wang, A., and Harris, T.N., 1996, Relative timing of fluid and anhydrite saturation: Another consideration in the sulfur budget of the Mount Pinatubo eruption, *in* Newhall, C.G., and Punongbayan, R.S., eds., Fire and Mud: Eruptions and Lahars of Mount Pinatubo, Philippines: Seattle, University of Washington Press, p. 875–891.
Putirka, K.D., 2008, Thermometers and barometers for volcanic systems: Reviews in Mineralogy and Geochemistry, v. 69, p. 61–120, https://doi.org/10.2138/rmg.2008.69.3.
Roedder, E., 1965, Liquid CO_2 inclusions in olivine-bearing nodules and phenocrysts from basalts: American Mineralogist, v. 50, p. 1746–1782.
Rust, A.C., Cashman, K.V., and Wallace, P.J., 2004, Magma degassing buffered by vapor flow through brecciated conduit margins: Geology, v. 32, p. 349–352, https://doi.org/10.1130/G20388.2.
Shamloo, H.I., and Till, C.B., 2019, Decadal transition from quiescence to supereruption: Petrologic investigation of the Lava Creek Tuff, Yellowstone Caldera, WY: Contributions to Mineralogy and Petrology, v. 174, 32, https://doi.org/10.1007/s00410-019-1570-x.
Tait, S., 1992, Selective preservation of melt inclusions in igneous phenocrysts: American Mineralogist, v. 77, p. 146–155.
Townsend, M., Huber, C., Degruyter, W., and Bachmann, O., 2019, Magma chamber growth during intercaldera periods: Insights from thermomechanical modeling with applications to Laguna del Maule, Campi Flegrei, Santorini, and Aso: Geochemistry, Geophysics, Geosystems, v. 20, p. 1574–1591, https://doi.org/10.1029/2018GC008103.
Vazquez, J.A., Kyriazis, S.F., Reid, M.R., Sehler, R.C., and Ramos, F.C., 2009, Thermochemical evolution of young rhyolites at Yellowstone: Evidence for a cooling but periodically replenished post-caldera magma reservoir: Journal of Volcanology and Geothermal Research, v. 188, p. 186–196, https://doi.org/10.1016/j.jvolgeores.2008.11.030.
Vigneresse, J.-L., Truche, L., and Richard, A., 2019, How do metals escape from magmas to form porphyry-type ore deposits?: Ore Geology Reviews, v. 105, p. 310–336, https://doi.org/10.1016/j.oregeorev.2018.12.016.
Waite, K.A., Keith, J.D., Christiansen, E.H., Whitney, J.A., Hattori, K., Tingey, D.G., and Hook, C.J., 1997, Petrogenesis of the volcanic and intrusive rocks associated with the Bingham Canyon porphyry Cu-Au-Mo deposit, Utah, *in* John, D.A., and Ballantyne, G.H., eds., Geology and Ore Deposits of the Oquirrh and Wasatch Mountains, Utah: Society of Economic Geologists Guidebook 29, p. 69–90.
Wallace, P.J., Anderson, A.T., Jr., and Davis, A.M., 1995, Quantification of pre-eruptive exsolved gas contents in silicic magmas: Nature, v. 377, p. 612–616, https://doi.org/10.1038/377612a0.

Printed in USA